Jurnal Teknologi

Full Paper

EFFECT OF Mn AND Ti ADDITION ON THE CRYSTALLOGRAPHIC STRUCTURE AND MAGNETIC PROPERTIES OF $SrFe_{12}O_{19}$

Wisnu Ari Adi[a], Yunasfi[a], Yosef Sarwanto[a], Muhammad Aziz Majidi[b]

[a]Center for Science and Technology of Advanced Materials National Nuclear Energy Agency of Indonesia (BATAN), Kawasan PUSPIPTEK Serpong, Tangerang – 15314
[b]Dept. of Physics, Faculty of Mathematics and Natural Sciences, University of Indonesia, Salemba Raya 4, Jakarta, Indonesia

Article history
Received
20 September 2019
Received in revised form
29 April 2020
Accepted
30 April 2020
Published online
22 June 2020

*Corresponding author
dwisnuaa@batan.go.id

Graphical abstract

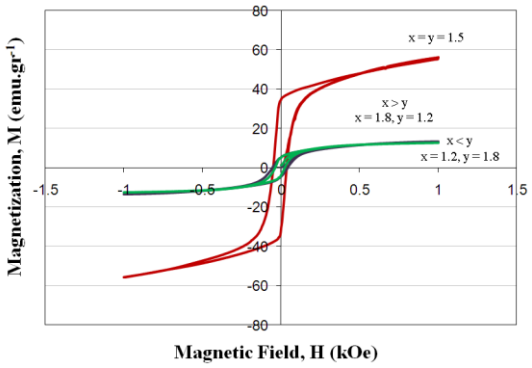

Abstract

The synthesis and characterization of composition $SrFe_{12-(x+y)}Mn_xTi_yO_{19}$ (x = y and x ≠ y) compound by using solid state reaction have been performed. The raw materials were $SrCO_3$, Fe_2O_3, $MnCO_3$, and TiO_2. The mixed powder was compacted at 5000 psi into pellets and sintered at 1050°C in the air at atmosphere pressure for 15 hours and furnace cooling. The refinement results of x-ray diffraction pattern show that the doping composition (x = y) was a single phase while the doping composition (x ≠ y) was multi phase. We concluded that effect of substitution upon magnetic properties revealed that total magnetization, remanence and coercivity changed with substitution due to preferential site occupancy of substituted Mn^{2+} and Ti^{4+} ions. The coercivity decreases with increase in Mn and Ti concentration. This effect is related with Fe^{3+} magnetic moment changes after they have already substituted Mn^{2+} and Ti^{4+} ions. Since the coercivity and total magnetization may be controlled by substitution while maintaining resistive properties, making this material useful for microwave absorber.

Keywords: Hexaferrite, substitution, manganese, titanium, phase, composition, and absorber

1.0 INTRODUCTION

The electronic device which working at high frequency is often has a problem on the emission of high frequency noise such as electromagnetic wave interference (EMI) [1-2]. To eliminate the EMI is required a magnetic material which able to resonate at a specific frequency that is expected to absorb electromagnetic radiation is undesirable. Recently electromagnetic absorbing materials are being developed is the modification of ferrite-based magnetic materials because it has a high permeability relatively [3-10]. The problem faced in a ferrite-based magnetic material that will be the object of this study is the magnetocrystalline anisotropy constant of this compound has relatively high value of ~ 330 kJ/m^3. This value is very high and causes the material has relatively large coercivity about ~ 1500 kA.m^{-1} which is needed as a permanent magnet [11-15]. However, as an absorber material of electromagnetic waves (microwave absorber) must have a coercivity value as low as possible so that the magnetic loss is low, but should still have a high value of the total magnetization. According to some literature it is mentioned that magnetic materials with the best absorption of microwaves, have a coercivity field of less than 1 kOe [1, 3, 4, 6-12]. As for the other properties necessary for electromagnetic wave absorbing material is a high permeability magnetic and resistive. Thus the material was necessary modified in order to reduce the value of coercivity while

maintaining the high value of the total magnetization. This will be tracked through the engineering crystal structure of the material.

According to González-Angeles et.al has reported that they have success to studied the structural and magnetic properties of $Ba_{0.5}Sr_{0.5}(ZnTi)_xFe_{12-2x}O_{19}$ (where x = 0.2 to 0.6) ferromagnetic powders prepared by mechanical milling. The obtained x-ray diffraction patterns Page 2 of 10 of Zn-Ti substituted $(Ba,Sr)_{0.5}M$ samples showed Magnetoplumbite phase formation for all substituted mixtures; no other secondary phases were detected. Scanning electron microscope analyses revealed that all processed samples possess particle size much below 1 µm and may exhibit promising magnetic and dielectric properties. Magnetic measurements showed that the intrinsic coercivity, Hci, and remanent magnetization, Mr, decreased as the substitution took place, while the saturation magnetization, Ms, remained almost constant (diminution ~ 9%). Hci, decreased from 389.92 down to 171.88 kA/m that represents a 56% drop, whilst Mr registered a fall of ~ 17%. [16]. Meanwhile Charanjeet et.al has reported that they have success to synthesize M-type hexagonal ferrite $Ba_{0.5}Sr_{0.5}Co_xRu_xFe_{(12-2x)}O_{19}$ (x = 0 to 1.2). The Co and Ru ions substitution cause increase in saturation magnetization and rapid decrease in magnetocrystalline anisotropy at lower substitution. The magnetic parameters variation has been explained by taking into account preferential site occupancy of sublattice sites by substituted ions. Curie temperature decreases with substitution due to weakening of superexchange interaction [17]. This study will be carried out strontium hexaferrite modification by manganese and titanium substituted iron atoms. Effect of substitution upon magnetic properties revealed that total magnetization, remanence and coercivity is also expected changed with substitution due to preferential site occupancy of substituted Mn^{2+} and Ti^{4+} ions. Since the coercivity and total magnetization is assumed able to be controlled by substitution, so required understanding about how much the maximum number of manganese and titanium atoms that able to substituting iron atom without changing the structure and its effect on the magnetic properties of this system. So the aims of this research synthesized strontium hexaferrite modification by manganese and titanium substituted iron atoms and understood changes in the phase and magnetic properties of this material.

2.0 METHODOLOGY

The synthesis of $SrFe_{12-(x+y)}Mn_xTi_yO_{19}$ (x = y and x ≠ y) material was performed by using the solid reaction method. This magnetic material is prepared by oxide materials, namely $SrCO_3$, Fe_2O_3, $MnCO_3$, and TiO_2, then weighed for each composition according to the stoichiometric rules following the reaction equation as follows:

$$SrCO_3 + (6\text{-}½(x+y))Fe_2O_3 + xMnCO_3 + yTiO_2 \rightarrow SrFe_{12-(x+y)}Mn_xTi_yO_{19} + (1+x)CO_2$$

The four of raw materials are mixed by using a high-energy milling (HEM) type Spex 8000 for 10 hours at room temperature. The finely mixed powder was compacted at 5000 psi into pellets and sintered in the electric chamber furnace THERMOLYNE at 1000°C in the air at atmosphere pressure for 10 hours.

The phase qualitative and quantitative of analysis were carried out using the PW1710 Philips diffractometer equipped (XRD), 30 kV tube voltage, 25 mA tube current, CuKα radiation (λ = 1.5406 Å), 2θ angle from 20° up to 80°, continuous-scan mode, step size of 0.02°, and time per step of 0.5 s. The Rietveld analysis was performed applying GSAS (general structure analysis system) program [18]. The surface morphology and element identification of the sample were analyzed by using the JEOL (JED-2300) scanning electron microscope (SEM) and energy dispersive spectroscopy (EDS), respectively. The magnetic properties were measured by vibrating sample magnetometer (VSM-OXFORD VSM1.2H) with external field from -1 up to 1 T.

3.0 RESULTS AND DISCUSSION

The identification results of measurements by x-ray diffraction on the samples show that the $SrFe_{12-(x+y)}Mn_xTi_yO_{19}$ (x = y = 0, 1.5, and 3) has been well established as shown in Figure 1.

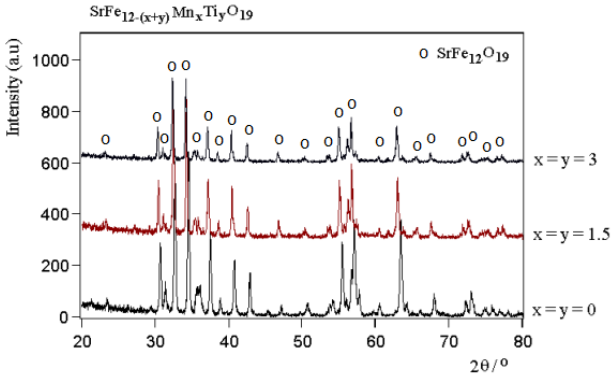

Figure 1 X-ray diffraction pattern of the $SrFe_{12-(x+y)}Mn_xTi_yO_{19}$ (x = y = 0, 1.5, and 3)

In Figure 1 shows that all the samples had been formed peaks are believed to have the same Miller index. The phase identification referred to the Crystallography Open Database (COD: 1008841). According to the Hanawalt table showed that the samples of $SrFe_{12-(x+y)}Mn_xTi_yO_{19}$ (x = y = 0, 1.5, and 3) can be identified as single phase. Since the Hanawalt table only can be used to qualitative analysis, the GSAS software is used for quantitative

analysis. In Figure 2 was shown the refinement result of x-ray diffraction pattern of $SrFe_{12-(x+y)}Mn_xTi_yO_{19}$ (x = y = 0, 1.5, and 3) samples.

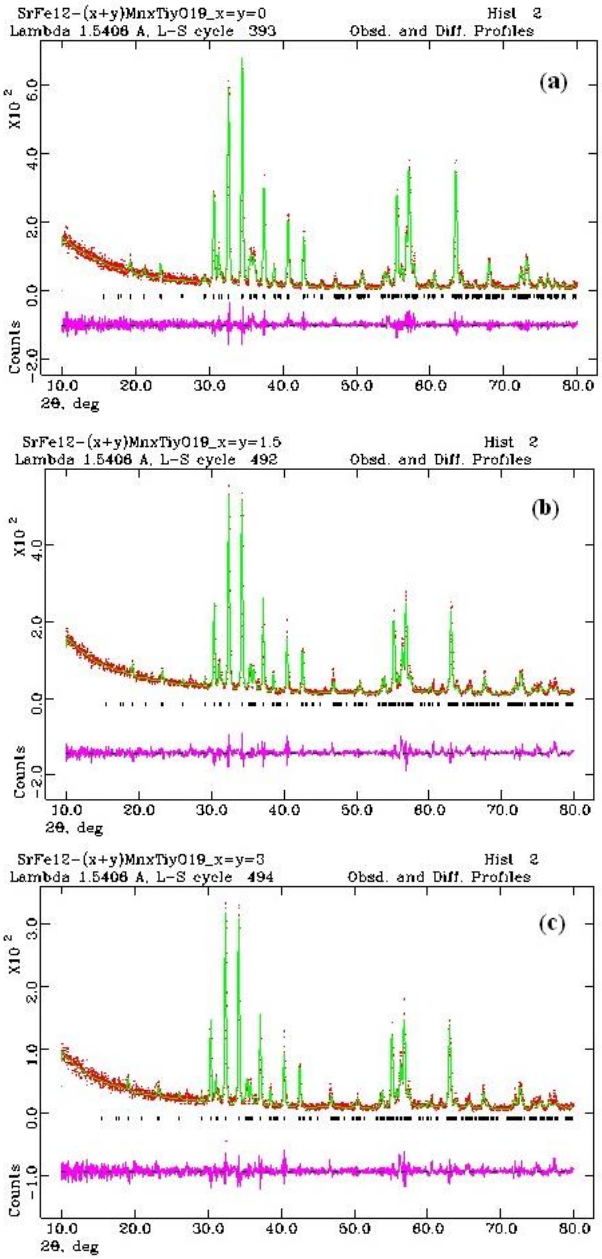

Figure 2 Refinement result of XRD pattern on $SrFe_{12-(x+y)}Mn_xTi_yO_{19}$ (a) x = y = 0, (b) x = y = 1.5, and (c) x = y = 3

The factors of quality of fitting of R (criteria of fit) χ^2 (goodness of fit) have been valued of minimum, and the allowed of χ^2 is less than 1.3. Figure 2 shows that the profile is in good agreement among the observation and calculations. The refinement results of x-ray diffraction pattern shows that the $SrFe_{12-(x+y)}Mn_xTi_yO_{19}$ (x = y = 0) sample is single phase with hexagonal structure, space group of P 63/m m c, the lattice parameters of a = 5.8849(2) Å, b = 5.8849(2) Å and c = 23.065(1) Å, α = β = 90° and γ = 89.63(1)°, V= 691.79(8) $Å^3$, ρ = 5.022 gr.cm^{-3}, wRp = 16.30, and χ^2 (chi-squared) = 1.297. Further confirmation was measuring the elemental analysis and observation of surface morphology on the samples to determine the particle distribution, homogenous, and its composition by using SEM-EDS equipment.

The elemental analysis and observation of surface morphology on the $SrFe_{12-(x+y)}Mn_xTi_yO_{19}$ shows that the sample has been well established as shown in Figure 3.

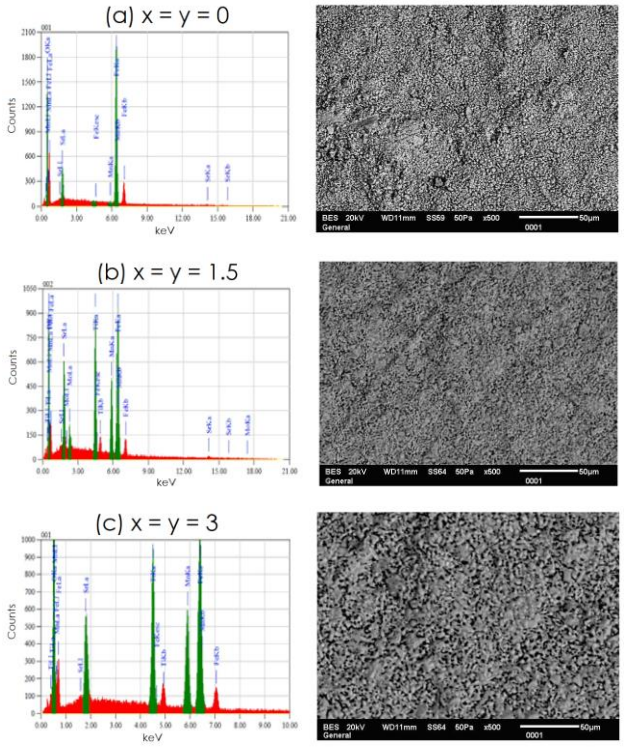

Figure 3 Surface morphology and elemental analysis of the $SrFe_{12-(x+y)}Mn_xTi_yO_{19}$

Figure 3 shows that all samples with the composition x = y have homogeneous and uniform particle shapes. This means that each sample with the composition x = y contains the same phase.

Table 1 The results of element analysis by using energy dispersive spectroscopy

Element	Content (wt.%)		
	x = y = 0	x = y = 1.5	x = y = 3
Strontium (Sr)	8.28 ± 0.29	8.24 ± 0.49	8.37 ± 0.19
Iron (Fe)	63.13 ± 0.26	45.32 ± 0.19	33.81 ± 0.19
Manganese (Mn)	-	8.96 ± 0.19	14.97 ± 0.19
Titanium (Ti)	-	8.94 ± 0.10	13.64 ± 0.10
Oxygen (O)	28.59 ± 0.10	28.54 ± 0.16	29.21 ± 0.15

So that required further analysis of the element content in the samples use energy dispersive spectroscopy. The elements content of the $SrFe_{12-(x+y)}Mn_xTi_yO_{19}$ are shown in Table 1.

EDS spectra shows that the sample had composition in accordance to stoichiometric composition. Therefore, these results need further confirmation by measurement of magnetic properties by using vibrating sample magnetometer to know the effect of substitution upon magnetic properties revealed that total magnetization, remanence and coercivity as shown in Figure 4.

The hysteresis loops in Figure 8 for $SrFe_{12-(x+y)}Mn_xTi_yO_{19}$ (x = y = 0, 1.5, and 3), and show the magnetic data and summarized in Table 2.

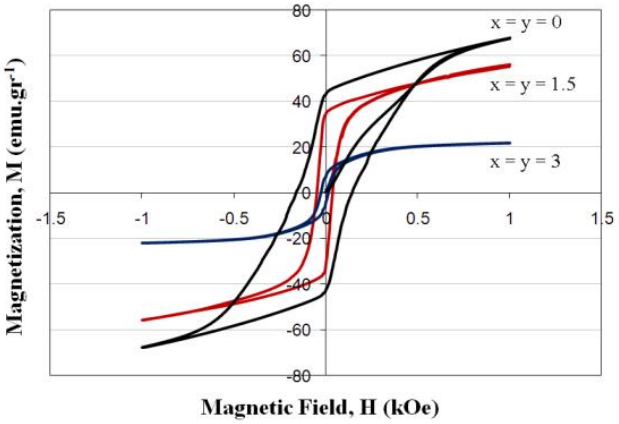

Figure 4 The hysteresis loops of the $SrFe_{12-(x+y)}Mn_xTi_yO_{19}$ (x = y = 0, 1.5, and 3)

The hysteresis loop consists of intrinsic saturation Ms, remanence Mr, and coercivity Hc. This saturation is the state when the material cannot absorb a stronger magnetic field such that an increase of magnetization force produces no significant change in magnetic flux density. The remanence Mr, for the samples shows the magnetization left behind in a medium after the external magnetic field has been removed, and coercivity also called the coercive force of a material is equal to the demagnetizing force required to reduce residual induction to zero in a magnetic field after magnetizing to saturation. Figure 4 appear that magnetic characterization show that the coercivity for x = 0 was 1510 Oe decrease drastically to 253 Oe for x = 0.3. In other hand that the coercivity decrease with increase in Mn and Ti concentration. This effect is related with Fe^{3+} magnetic moment changes after they have already substituted Mn^{2+} and Ti^{4+} ions.

Table 2 Summary of magnetization measurement for x = y samples

Composition (x)	Magnetic parameter		
	Ms (emu/g)	Mr (emu/g)	Hc (Oe)
0.0	67.37	45.03	1510
1.5	57.51	38.97	428
3.0	21.38	10.01	253

An absorber material of electromagnetic waves (microwave absorber) must have a coercivity value as low as possible so that the magnetic loss is low, but should still have a high value of the total magnetization. It means that the sample have a low coercivity and high magnetization is $SrFe_{12-(x+y)}Mn_xTi_yO_{19}$ (x = y = 1.5).

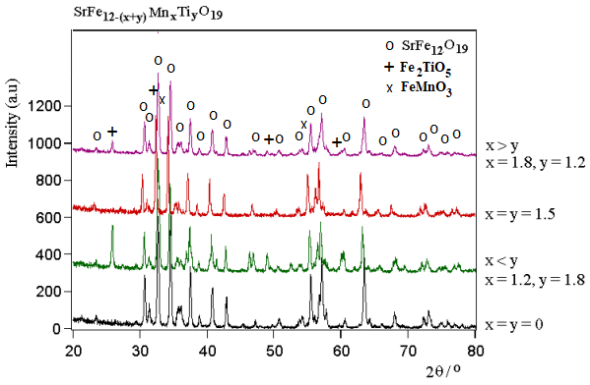

Figure 5 X-ray diffraction pattern of the $SrFe_{12-(x+y)}Mn_xTi_yO_{19}$ (x = y, x < y and x > y)

However how much the maximum number of manganese and titanium atoms (x = y and x ≠ y) that able to substituting iron atom without changing the structure and its effect on the magnetic properties of this system. Therefore in Figure 5 is showed the result of XRD measurement on the $SrFe_{12-(x+y)}Mn_xTi_yO_{19}$ (x = y, x < y and x > y, with x + y = 3).

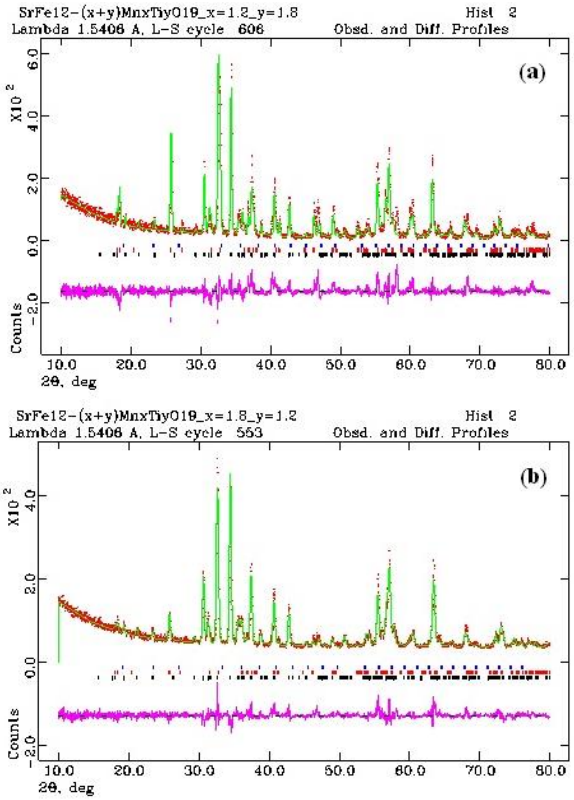

Figure 6 Refinement result of XRD pattern on $SrFe_{12-(x+y)}Mn_xTi_yO_{19}$ (a) x < y and (b) x > y

In Figure 5 shows that the samples had been formed peaks are believed to have the same Miller index for x = y, however it was found unknown peaks for x < y and x > y. In Figure 2 was shown the refinement result of x-ray diffraction pattern of $SrFe_{12-(x+y)}Mn_xTi_yO_{19}$ (x < y and x > y) samples.

Figure 6 showed that the profile is also in good agreement among the observation and calculations. The refinement results of X-ray diffraction pattern shows that the $SrFe_{12-(x+y)}Mn_xTi_yO_{19}$ shows a single phases for x = y and the sample is multi phase for x < y and x > y.

This result is in accordance to the calculation results of the mass fraction as shown in Table 3.

Table 3 Mass fraction of the $SrFe_{12-(x+y)}Mn_xTi_yO_{19}$ (x < y and x > y) samples

Sample	Phase	Mass fraction	wRp	χ^2
x < y x = 1.2 and y = 1.8	$SrFe_{12}O_{19}$	67.03 %	20.38	1.306
	Fe_2TiO_5	31.87 %		
	$FeMnO_3$	1.11 %		
x > y x = 1.8 and y = 1.2	$SrFe_{12}O_{19}$	65.38 %	18.56	1.249
	Fe_2TiO_5	2.79 %		
	$FeMnO_3$	31.83 %		

The elemental analysis and observation of surface morphology on the $SrFe_{12-(x+y)}Mn_xTi_yO_{19}$ (x < y and x > y) are shown as in Figure 7.

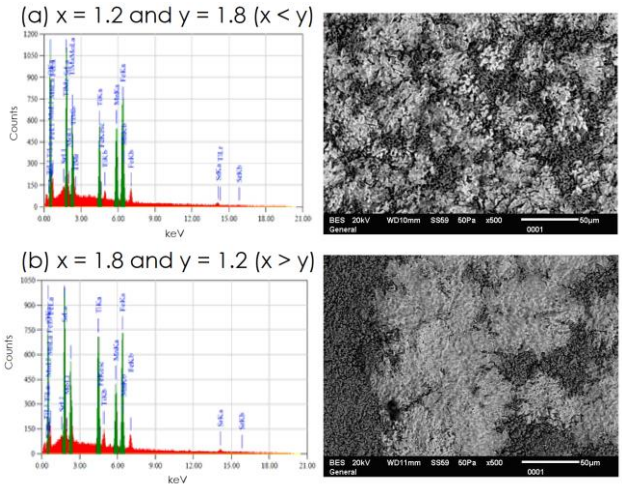

Figure 7 Surface morphology and elemental analysis of the samples (x < y and x > y)

The elements content of the $SrFe_{12-(x+y)}Mn_xTi_yO_{19}$ (x < y and x > y) are shown in Table 4.

Table 4 The results of element analysis by using energy dispersive spectroscopy

No.	Element	Content (wt.%)	
		x = 1.2 and y = 1.8 (x < y)	x = 1.8 and y = 1.2 (x > y)
1.	Strontium (Sr)	8.38 ± 0.15	8.04 ± 0.13
2.	Iron (Fe)	42.49 ± 0.16	44.46 ± 0.14
3.	Manganese (Mn)	7.55 ± 0.16	10.39 ± 0.14
4.	Titanium (Ti)	9.01 ± 0.09	6.03 ± 0.08
5.	Oxygen (O)	32.57 ± 0.16	31.08 ± 0.10

EDS spectra shows that the dominant elements were strontium (Sr), iron (Fe), manganese (Mn), titanium (Ti), and oxygen (O). The microstructure observation shows that the particles consist of the varied shapes. It means that the microstructure result supported the XRD result that the samples are suspected consist of more than one phase. Therefore, these result is also required further confirmation by measurement of magnetic properties by using vibrating sample magnetometer to know the effect of x and y composition on the magnetic properties revealed that total magnetization, remanence and coercivity as shown in Figure 8.

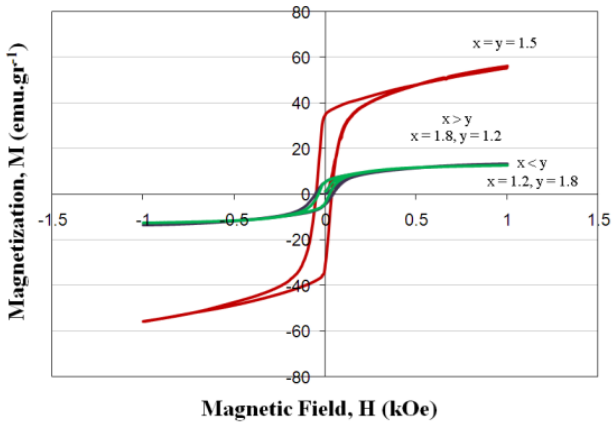

Figure 8 The hysteresis loops of the $SrFe_{12-(x+y)}Mn_xTi_yO_{19}$ (x = y and x ≠ y).

The magnetic data and summarized was shown in Table 5.

Table 5 Summary of magnetization measurement for x ≠ y samples

Sample	Magnetic parameter		
	Ms (emu/g)	Mr (emu/g)	Hc (Oe)
x = 1.2 and y =1.8	13.24	6.42	343
x = 1.2 and y = 1.8	13.20	6.41	258

Figure 8 appear that magnetic characterization show that the remanence for x = y = 1.5 was 38.97 emu/gr decrease drastically to 6.42 emu/gr for x ≠ y. In other hand that the remanence decrease with change in Mn and Ti composition. It is suspected that there is a hexagonal ferrite phase in the particles but the presence was not confirmed in the x-ray diffraction profile, presumably due to its extremely small fraction.

4.0 CONCLUSION

In this research has successfully synthesized sample of $SrFe_{12-(x+y)}Mn_xTi_yO_{19}$ (x = y and x ≠ y). In this study has managed to understand the characteristics of the iron atom substitution in the manganese atoms in the $SrFe_{12-(x+y)}Mn_xTi_yO_{19}$ (x = y and x ≠ y). The refinement results of x-ray diffraction pattern showed that the doping composition (x = y) was a single phase while the doping composition (x ≠ y) was multi phase. the substitution increases density and inter grain connectivity in the microstructure of sintered samples. Effect of substitution upon magnetic properties revealed that total magnetization, remanence and coercivity changed with substitution due to preferential site occupancy of substituted Mn^{2+} and Ti^{4+} ions. The coercivity decreases with increase in Mn and Ti concentration. This effect is related with Fe^{3+} magnetic moment changes after they have already substituted Mn^{2+} and Ti^{4+} ions. Since the coercivity and total magnetization may be controlled by substitution while maintaining resistive properties, making this material useful for microwave absorber.

Acknowledgement

Many thank to Drs. Bambang Sugeng, Dra. Mujamilah, M.Sc., and Dra. Deswita for their kind help to characterize using XRD, VSM, and SEM-EDS, respectively. Author contributions: Wisnu Ari Adi and Yunasfi designed research, performed research, analyzed data, and wrote the paper. Both authors approved the final manuscript and contributed equally to be the paper.

References

[1] Wisnu Ari Adi, Yunasfi Yunasfi, Mashadi Mashadi, Didin Sahidin Winatapura, Ade Mulyawan, Yosef Sarwanto, Yohanes Edi Gunanto, Yana Taryana. 2019. Electromagnetic Fields and Waves. *Metamaterial: Smart Magnetic Material for Microwave Absorbing Material*. United Kingdom: IntechOpen Limited. DOI: http://dx.doi.org/10.5772/intechopen.84471.

[2] Magham, S. B. S., Sharma, M., Shannigrahi, S. R., RuTan, H., Sharma, V., Meng, Y. S., Idapalpati, S., Ramanujan, R. V., Repaka, D. V. M. 2017. Development of Z-type Hexaferrites for High Frequency EMI Shielding Applications. *Journal of Magnetism and Magnetic Materials*. 441: 303-309. DOI: 10.1016/j.jmmm.2017.05.066.

[3] Nikmanesh, H., Moradim, M., Bordbar, G. H., Alam, R. S. 2017. Effect of Multi Dopant Barium Hexaferrite Nanoparticles on the Structural, Magnetic, and X-Ku Bands Microwave Absorption Properties. *Journal of Alloys and Compounds*. 708: 99-107. https://doi.org/10.1016/j.jallcom.2017.02.308.

[4] Afghahi, S. S. S., Jafarian, M., Salehi, M., Atassi, Y. 2017. Improvement of the Performance of Microwave X Band Absorbers Based on Pure and Doped Ba-hexaferrite. *J. Magn. Magn. Mater*. 421: 340-348. http://dx.doi.org/10.1016/j.jmmm.2016.08.042.

[5] Yunasfi Y., Wisnu A. A., Mashadi M., Rahmy, P. A. 2017. Magnetic and Microwave Absorption Properties of Nickel Ferrite (NixFe3-xO4) by HEM Technique. Malaysian *Journal of Fundamental and Applied Sciences (MJFAS)*. 13: 203-206. DOI: https://doi.org/10.11113/mjfas.v13n3.553.

[6] Shams, M. H., Rozatian, A. S. H., Yousefi, M. H., Valíček, J., Šepelák, V. 2016. Effect of Mg^{2+} and Ti^{4+} Dopants on the Structural, Magnetic and High-Frequency Ferromagnetic Properties of Barium Hexaferrite. *J. Magn. Magn. Mater*. 399: 10-18. https://doi.org/10.1016/j.jmmm.2015.08.099.

[7] Manawan, M., Manaf, A., Soegijono, B. & Yudi, A. 2014. Microstructural and Magnetic Properties of Ti^{2+}-Mn^{4+} Substituted Barium Hexaferrite. *Adv. Mater. Res.* 896: 401-405. https://doi.org/10.4028/www.scientific.net/AMR.

[8] Yohanes Edi Gunanto, Eric Jobiliong, Wisnu Ari Adi. 2016. Microwave Absorbing Properties of Ba0.6Sr0.4Fe12-zMnzO19 (z=0–3) Materials in X-Band Frequencies, *Journal of Mathematical and Fundamental Sciences*. 48(1): 55-65. DOI: http://dx.doi.org/10.5614%2Fj.math.fund.sci.2016.48.1.6.

[9] José Eves M. Silva, Ricardo S. Nasar, Marinalva C. Nasar, Caio L. Firme, José H. Araújo. 2015. Correlation between Coercive Field and Radiation Attenuation in Ni and Mg Ferrite Doped with Mn and Co. *Journal of Magnetism and Magnetic Materials.* 394: 274-279. https://doi.org/10.1016/j.jmmm.2015.06.014.

[10] Singh, J., Singh, C., Kaur, D., Narang, S. B., Joshi, R., Mishra, S. R., Jotania, R., Ghimire, M,. Chauhan, C. C. 2016. Tunable Microwave Absorption in Co/Al Substituted M-Type Ba/Sr Hexagonal Ferrite. *Mater.* 110: 749-761. DOI: 10.1016/j.matdes.2016.08.049.

[11] Vinnik, D. A., Yu. A., Tarasova, Zherebtsov, D. A., Gudkova, S. A., Galimov, D. M., Zhivulin, V. E., Trofimov, E. A., Nemrava, S., Perov, N. S., Isaenko L. I., and Niewa, R., 2017. Magnetic and Structural Properties of Barium Hexaferrite $BaFe_{12}O_{19}$ from Various Growth Techniques, *Materials*. 10(6): 578. DOI:10.3390/ma10060578.

[12] Li Deng, Yang Zhao, Zhaoming Xie, Zuohua Liu, Changyuan Tao and Rongrui Deng. 2018. Magnetic and Microwave Absorbing Properties of Low-temperature Sintered BaZrxFe(12−x)O19. *RSC Adv*. 8: 42009-42016. DOI: 10.1039/c8ra08783k.

[13] Shafqat, M. B., Arif, O., Atiq, S., Saleem, M., Ramay, S. M., Mahmood, A., Naseem, S. 2016. Influence of Sintering Temperature on Structural, Morphological and Magnetic Properties of Barium Hexaferrite Nanoparticles. *Mod. Phys. Lett. B*. 30: 1650254. https://doi.org/10.1142/S0217984916502547.

[14] Putra, K. P. and Manaf, A. 2017. Structural and Magnetic Properties of (Ba1-xLax)Fe12O19 Obtained by Mechanical Alloying and Ultrasonic Irradiation. *AIP Conference Proceedings* 1862: 030055. DOI: 10.1063/1.4991159.

[15] Tudorache, F., Popa, P. D., Brinza, F., Tascu, S. 2012. Structural Investigations and Magnetic Properties of $BaFe_{12}O_{19}$ Crystals. *Acta Phys. Pol. A*. 121: 95-97.

[16] González-Angeles, A., Grusková, A., Lipka, J., Sláma, J. and Jančárik. V. 2008. Magnetic and Structural Studies of $Ba_{0.5}Sr_{0.5}(ZnTi)_xFe_{12-2x}O_{19}$ Prepared by Ball Milling. *Jordan Journal of Phys.* 1: 1: 37-42.

[17] Singh, C., Narang, S. B., Hudiara, I. S., Bai, Y., Tabatabaei, F., 2008. Static Magnetic Properties of Co and Ru Substituted Ba–Sr Ferrite. *Materials Research Bulletin.* 43: 176-184. https://doi.org/10.1016/j.materresbull.2007.06.050.

[18] Idris, M. S., Osman, R. A. M. 2013. Structure Refinement Strategy of Li-Based Complex Oxides Using GSAS-EXPGUI Software Package. *Advanced Materials Research.* 795: 479-482. Doi:10.4028/www.scientific.net/AMR.795.479.